

HYBRIDIZATION OF SIMULATION CODES BASED ON NUMERICAL HIGH AND LOW FREQUENCY TECHNIQUES FOR THE EFFICIENT ANTENNA DESIGN IN THE PRESENCE OF ELECTRICALLY LARGE AND COMPLEX STRUCTURES

H.-T. Chou and H.-T. Hsu

The Department of Communications Engineering
and Communication Research Center
Yuan Ze University
135 Yuan-Tung Rd., Chung-Li 320, Taiwan

Abstract—A hybridization approach to integrate simulation codes based on high and low frequency techniques is developed in this paper. This work allows the antenna design to be performed directly in the presence of the complex and large structures. Since the sizes of the complex structures can be extremely large electrically, and the antenna structure itself can be significantly complicated, such problems can not be resolved with a single technique alone. While low frequency techniques are generally applied for antenna design problems where small scale interactions are involved, high frequency techniques are adopted for the prediction of propagation effects inside the complex structures. The proposed hybridization approach provides a seamless integration of low and high frequency techniques that combines the advantages of both techniques in terms of accuracy and efficiency. Numerical example is presented to demonstrate the utilization of the proposed approach.

1. INTRODUCTION

The fast growing of wireless communications has spurred increasing possibility of using antennas under electrically large structures such as cars or aircrafts. Antennas designed directly in the presence of these large structures are thus of interest because the overall antenna performance can be relatively considered. However, the difficulty of antenna analysis and numerical simulation for such cases is drastically increased since the structure can be extremely large and complex. Note

that these problems generally involve with the analysis of small scale electromagnetic (EM) field interactions within the antenna structure and the large scale EM propagation predictions due to the antenna radiation within the structures. Apparently conventional approaches of high or low frequency techniques can not be used alone to treat such antenna design problems, a lot of recent developments have highlighted the necessity of using hybrid methods [1–3] to solve such problems. Specifically, low frequency (LF) techniques such as finite element method (FEM) [4], finite difference time domain (FDTD) [5] and method of moment (MoM) [6] have been shown suitable to analyze the small scale interactions within the antenna structure, but are not effective to analyze the large scale propagation problems due to the limitation of computational power. On the other hand, however, high frequency (HF) techniques [7–9] such as uniform geometrical theory of diffraction (UTD) [7], physical-optics method [10, 11], other diffraction or scattering methods [12–16] are capable of analyzing large scale propagation problems in the presence of electrically large and complex structures by using ray tracing techniques, but are not capable of analyzing the small scale interactions within the antenna because of the difficult ray tracing to achieve accurate results. Thus an effective approach to hybridize the high and low frequency techniques and create an useful tool may significantly assist the engineers to resolve this design problem.

The hybridization of high and low frequency techniques has been proposed and studied for decades [17–20], with most works dedicated to either assist HF techniques to increase the accuracy in predicting the wave propagations within a large structure [17] or to assist LF techniques in reducing the number of unknowns to be solved [18]. In particular, most of the works are related to either scattering problems or radiation problems associated with simple antenna structures (such as wire antennas [19, 20]). Not much of the works, especially in terms of publicly available software, can be effectively applied to general antenna design problems in the presence of electrically large and complex structures especially when antenna design optimization is necessary, resulting in a large number of repeated analysis.

Based on commercially available codes, the proposed approach provides a relatively simple way to resolve the antenna design problems in the presence of large and complex structures. The reliability of analysis is assured to a certain degree except the errors incurred due to interactions between codes. Thus, in situations where the interactions do not impact the results, effective antenna designs can be achieved. Furthermore, the proposed approach may essentially extend the limitations of individual codes when used alone. It is noted

that recently a domain decomposition method [21] has been proposed to decompose a big electromagnetic problem into small sub-domain problems and account for the interactions between sub-domains, whose concepts may be applied to reduce the errors and will be performed in the next phase of this work.

To demonstrate the concepts of code hybridization, NEC-BSC [22] and CST Microwave Studio (MWS) [23] are identified as the HF and LF techniques, respectively in the following development. Since CST MWS is a true three dimensional exact full wave electromagnetic solver based on the Finite Integration Technique (FIT) in time domain, the accuracy of this work relies on the computation of NEC-BSC, a UTD based code with a certain degree of approximation, and the interaction between these two codes. An interface to decompose the antenna design problems into sub-domains of each code is established and performs the parameter transformations between the codes. In particular, the concepts of generalized ray expansion (GRE) method [24, 25] are applied in the interface establishment. The advantages of the GRE are that the propagation predictions using a ray tracing technique need to be performed only once regardless the antenna types if the large structure of interest remains unchanged. It is particularly useful for antenna design optimization since during the procedure of optimization each change on the antenna structure needs to be considered only as a new antenna analysis.

2. IMPLEMENTATION STRATEGIES

The problem under consideration is the antenna design within a large and complex structure as illustrated in Figure 1, where several electrically large and complex platforms of interest are shown. The antenna can be a single element or an array to radiate required patterns that fulfills the specified requirements. Thus this antenna



Figure 1. Several electrically large and complex structures of interest, including satellite, helicopter and aircraft. Antennas are to be designed in the presence of such structures.

design problem exhibits two considerations including the electric characteristics, such as the bandwidth of return loss, and radiation characteristics such as the radiation patterns, axial ratios and cross-polarization levels. As the bandwidth of the antennas is primarily affected by small scale wave interactions within the antenna structures, the radiation characteristics will be impacted by the propagations of the radiated fields through the large and complex antenna platforms. Thus if the problem is properly decomposed into two sub-domains suitable to be analyzed by HF and LF techniques, respectively, the problems can be approximately resolved. The basic implementation process starts from decomposition of the complex problem into HF and LF sub-domains through proper domain decomposition of the structure. While the basic electric characteristics associated with the antennas are taken care of by LF techniques, HF techniques take care of the prediction of propagations of the large structure. The antenna is basically designed in the LF sub-domain and the corresponding field distributions together with the induced currents on the pre-defined virtual boundaries are obtained and transformed into HF sub-domain. Principle of equivalence is then applied with properly assigned enclosures on the virtual boundaries in the HF sub-domain to predict the propagation characteristics of the overall structure.

2.1. Problem Decomposition into HF and LF Sub-domains

The antenna design problem as illustrated in Figure 1 may be decomposed into two sub-domains that can be analyzed by NEC-BSC and CST MWS, respectively, referred as the BSC and CST sub-domains, respectively. Since CST is effective to analyze the small scale interactions within the antenna structure, it is nature to define a CST sub-domain with respect to the region in the vicinity of the antenna structure. Thus it is assumed that the components of the complex structure far away from the antenna do not significantly impact the antenna's electric characteristics in this work. It is approximately valid for those components that are at least 2 wavelengths away from the antenna and do not directly block the antenna radiation, which generally fulfills the situations of practical applications. Thus a straightforward decomposition approach cuts the antenna vicinity region as the CST sub-domain, as illustrated in Figure 2(a), for the analysis of the antenna design. The size of the CST sub-domain may be as large as to the limit that CST may handle. Thus in the cases that the portions of the complex structure are near the antenna and directly block the antenna radiation, they may be included in the region of CST sub-domain. At this stage, the analysis of CST sub-domain is merely a problem of an antenna design in the presence of a small

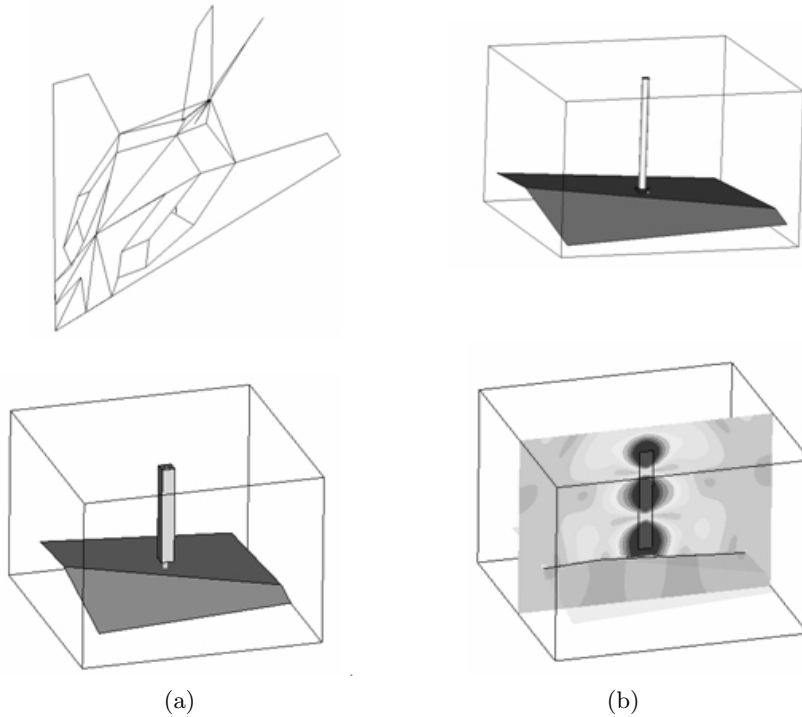


Figure 2. (a) Illustration of BSC (left) and CST (right) sub-domain decomposition, where in BSC HF sub-domain, the antenna is mounted on the wing of the jet fighter; (b) The enclosed surface with calculated absolute value of equivalent currents in LF (CST) sub-domain.

decomposed structure with additional impacts due to the diffractions from the artificial cutting edges which are not supposed to occur in the original problem. Note that if the edge diffractions may be properly removed or reduced, the electric characteristics of antenna, such as return loss and induced currents, remain relatively accurate in the analysis of CST sub-domain. Note that at present stage the far field radiation of the antenna is not of major concern since the antenna radiation will experience propagations through the complex structure and arise to the patterns of interest in this work.

The establishment of the BSC sub-domain is based on an equivalence principle model (or Love's Equivalence principle) to equivalently replace the antenna by induced currents on a surface enclosing the antenna as illustrated by S in Figure 2(b). It is noted that since the impact due to the scattering from far-end components

of the complex structure is ignored in this work, the total fields on are approximately the near fields radiated from the antenna designed in CST sub-domain and in presence of the structures inside CST sub-domain. The size of the surface should be selected in a way that the components with small scale interactions near the antenna structure to be enclosed so that UTD solutions for the fields radiated from equivalent currents remain valid when the fields first illuminate the remaining components of the complex structure. Also the region inside S is perfectly electrically conducting and has a null fields. The induced currents on S are magnetic and can be described as

$$\overline{M}_s = -\hat{n} \times \overline{E}_a \quad (1)$$

where \hat{n} is a unit vector normal to S and E_a is the near electrical field radiated from the antenna in presence of the structure inside the CST sub-domain. It is noted that it is important to make the body enclosed by S electrically conducting so that the fields inside S may be retained null and the equivalent currents are directly on the surface of S during the analysis of NEC-BSC as required in the equivalence principle. In general, for specific applications, it is better to keep smoothly varying, such as a half sphere, such that redundant errors may be better minimized due to the numerical integration over currents in NEC-BSC.

2.2. Treatment for CST to Reduce Artificial Edge Diffractions

The establishment of CST sub-domain will produce artificial edge truncations on the portion of the complex structure to be included in the sub-domain. Redundant diffractions will occur from the artificial edges. They should be reduced in order not to impact significantly on the electrical characteristics of the antenna under design inside the CST sub-domain. This reduction is achieved by properly imposing tapered absorbers on the edge truncations. Note that even though absorbing boundary conditions are commonly employed in LF techniques and are also available in CST, they are not capable of reducing the edge diffractions. It is because the absorbing boundary conditions employ multi-layer materials with tapered values of resistance so that the reflections from the boundaries into the analysis domain may be minimized, which means that resistance near the interface of the analysis domain is quite small and will not be capable of reducing significantly the diffractions occurred from the edges inside the analysis domain. The illustration of imposing resistance-tapered absorbers is shown in Figure 3, where the resistance-tapered absorbers are realized

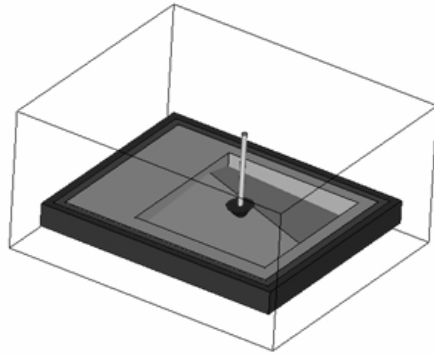


Figure 3. Tapered absorbers wrapping around the artificial edges to minimize the diffraction.

by multi-layer materials as that employed in the absorbing boundary conditions except now the edge truncations are inside boundary. This allows the antenna's radiating fields to be attenuated while propagating through the tapered absorbers to illuminate the edges. While such technique seems to be very straightforward intuitively, care must be taken in practical implementation. Since the absorbing materials are frequency-dependent and consist of relatively high-dielectric materials with loss, inclusion of the absorbing material into the calculation domain often increases the number of mesh cells within the calculation domain, leading to a longer simulation time. Alternatively, if the artificial edges of the decomposed structure are regular (namely, lining up with the axes of boundary planes), the artificial edges could be removed by utilization of several PML layers with increased sub-domain size during decomposition process.

2.3. Implementation of GRE Interface

The integration between these two codes can be realized only when the interface is well established. The GRE concept is illustrated in Figure 3 and implemented in this work for the interface. The advantages of the GRE are that the analysis of propagation based on ray tracing techniques needs computed only once regardless the changes of the antennas, which dramatically saves the computational time when different types of antennas will be used. The implementation of the concepts is based on basis expansions of the current distributions over

S in Figure 2, i.e.,

$$\overline{M}_s = \sum_{n=1}^N A_n \overline{M}_n \quad (2)$$

where N basis functions are used. As the current distributions, \overline{M}_s , change with respect to the change of the antenna enclosed by S only the weighting coefficient, A_n , related to each basis will change since the basis functions remain same. Each basis, \overline{M}_s , serves as the source to be used in NEC-BSC, where its radiation is represented in terms of a set of rays, to compute the scattering fields in presence of the complex structures. The ray parameters and their associated scattering field remain fixed as the complex structure remains unchanged. NEC-BSC allows users to use several types of current sources (either electric or magnetic sources) including uniform, piecewise sinusoidal, TE₀₁ cosine, annular ring, constant circular and TE₁₁ circular current distributions, among which uniform (or pulse) and piecewise sinusoidal current distributions have been widely used in numerical techniques as basis functions to represent induced currents and can be used in (2) to represent the current distributions on S . Thus let \overline{E}_{nm} be the scattering fields at m th observation point due to \overline{M}_n , the total scattering fields at m th observation point due to the antenna radiation can be expressed as

$$\overline{E}_m = \sum_{n=1}^N A_n \overline{E}_{nm}. \quad (3)$$

Thus if \overline{E}_{nm} are pre-computed and stored in the memory, they can be used to efficiently compute the scattering fields due to the antenna radiation regardless the changes of antennas since \overline{E}_{nm} need to be found only once. It is noted that this strategy allows the users to concentrate their efforts on designing the antenna using LF techniques.

2.4. Numerical Example

The proposed approach is validated by considering an antenna design in the presence of a car structure, where the antenna is a monopole and mounted on the car's roof for the simplification of demonstration. The structure and its dimensions are illustrated in Figure 5(a). Figure 5(b) shows the meshed view at a specific plane of interest. To validate the analysis accuracy of this work, the frequency of operation is assumed to be 900 MHz in the mobile communications, which allows the structure analyzable by LF codes, namely CST, alone. Its results will be used as a reference solution for the comparison of accuracy with the solution obtained by the proposed approach.

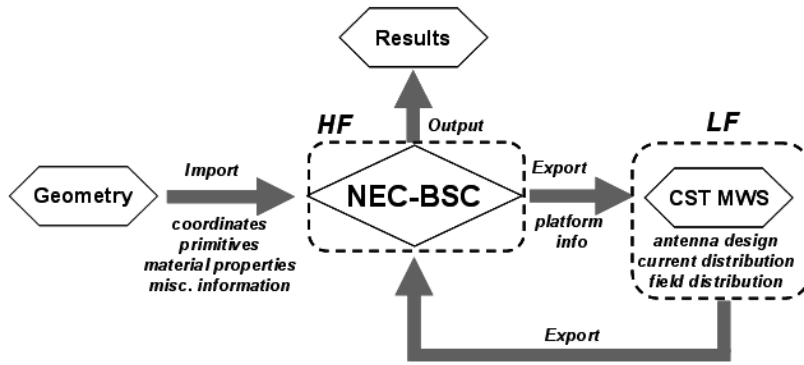


Figure 4. The flow chart illustrates the procedure of establishing code integration.

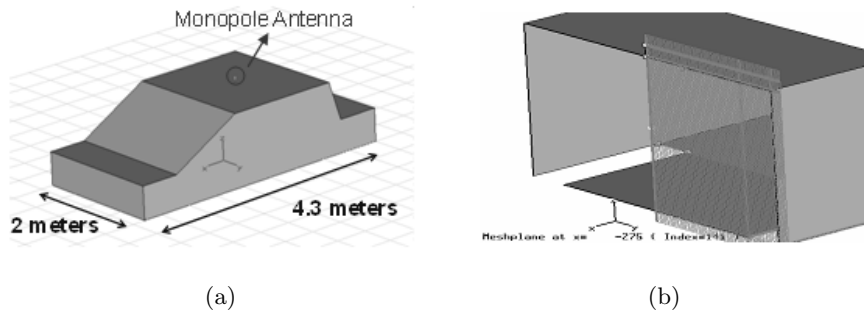


Figure 5. (a) The structure and dimensions of a car structure, where the monopole antenna is mounted on top of the car. (b) Mesh view at a specific plane in CST.

Since FIT based CST Microwave Studio adopted the explicit algorithm without any matrix inversion process involved, generally it is capable of handling relatively larger problems compared to other commercially available codes. The whole structure of interest was analyzed in CST and the calculated S_{11} with 3-D far field radiation pattern are shown in Figure 6. The total number of mesh cells is 4,489,017 in this specific case, with proper symmetry plane set to efficiently save the computational resources in terms of mesh cells and computation time which is recorded to be 65 minutes on an Intel Xeon™ 3.40 GHz CPU with 3 GB RAM desktop. The calculated far field response will serve as a reference to compare with that calculated

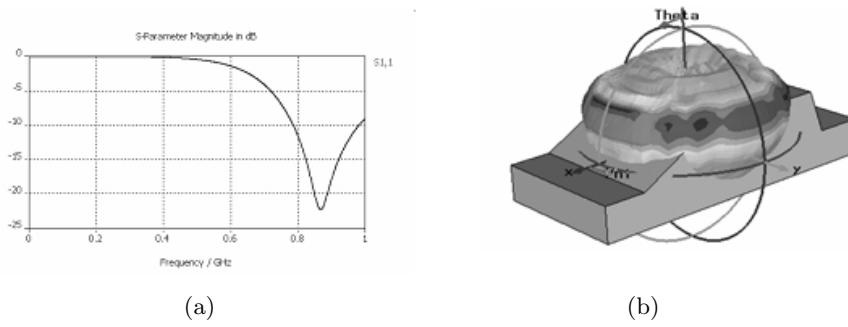


Figure 6. Simulated (a) S_{11} and (b) 3-D farfield radiation pattern of the 900 MHz monopole antenna mounted on the top of the car by CST MWS.

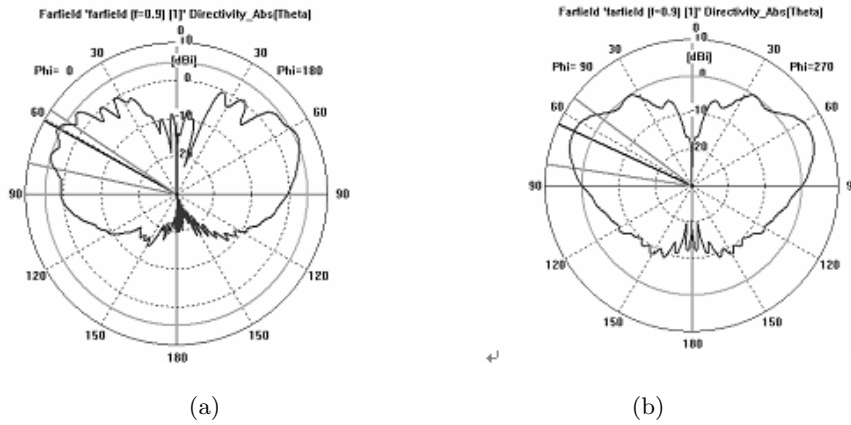


Figure 7. Polar plots of the corresponding radiation at (a) $\phi = 0^\circ$ and (b) $\phi = 90^\circ$.

by our approach. Figure 7 shows the corresponding polar plots at $\phi = 0^\circ$ and 90° , respectively.

The overall structure is decomposed into LF and HF sub-domains and Figure 8 shows the decomposed structure in LF sub-domain. A predefined virtual box with size $0.05\lambda \times 0.05\lambda \times 0.25\lambda$ that encloses the antenna is also shown in the figure. Based on the principle of equivalence, electric fields on the enclosing surfaces will then be calculated and converted into the surface magnetic currents to be imported into the HF sub-domain for propagation prediction.

In our specific example here, a larger decomposed domain is

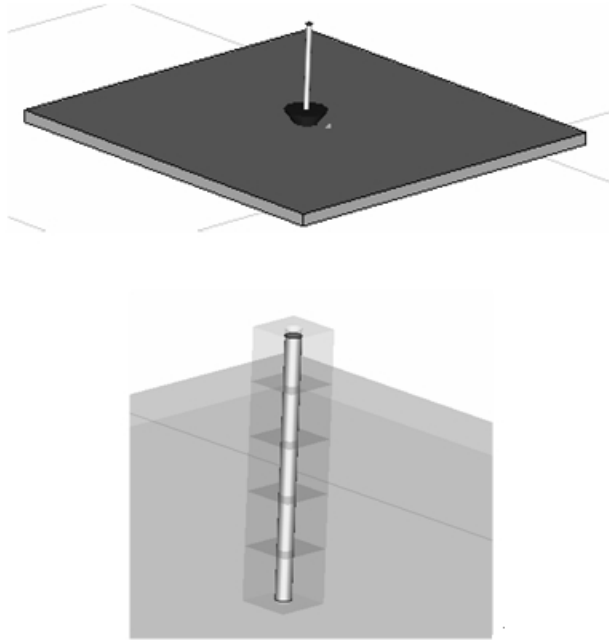


Figure 8. The decomposed structure in LF sub-domain with the enclosed surface for electric field calculation.

adopted instead of the tapered absorbing material to reduce the diffractions by the artificial edges. The reason of doing so is merely to save the computation time and effort by avoiding very dense meshing at the absorbing materials. Under such circumstances where a larger decomposed sub-domain is adopted, four PML layers with specified reflections that touch the decomposed edges directly can be used instead of the absorbing boundaries. Convergence test is firstly performed to make sure that the size of decomposition domain is large enough. Figure 9 shows the probed field quantities with various sizes of the sub-domains. As is concluded from the test, the near field behaviors of the antenna of interest become independent of the touching boundaries if they are at least one wavelength away from the antenna's location. Figure 10 shows the transformed current distribution at the corresponding location in HF sub-domain to be analyzed by NEC-BSC code. The virtual boundaries in LF sub-domain are now replaced by PEC enclosures in HF sub-domain since we are dealing with magnetic currents. Finally the propagation predictions are performed using NEC-BSC code and the resulted far field pattern is

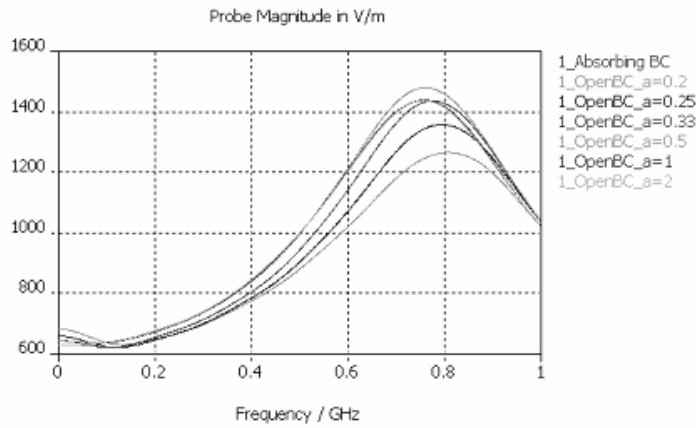


Figure 9. Probed electric field with various sizes of the decomposed sub-domains showing that the results become independent of the touching boundaries if the size is at least one wavelength away from the antenna location.

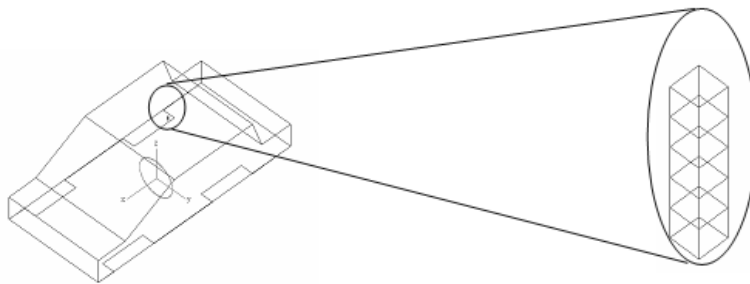


Figure 10. The transformed current distribution at the corresponding location in HF sub-domain to be analyzed by NEC-BSC code.

shown in Figure 11 with that calculated directly from CST Microwave Studio included for comparison. In this case, only 2 minutes CPU time was used in CST to compute the results in LF sub-domain and the CPU time used in NEC-BSC is ignorable in this case. Note that only the pattern is of interest for comparison because the values should depend on the choice of observation location. It is clear that the results agree very well with each other evidencing the correctness of the proposed approach.

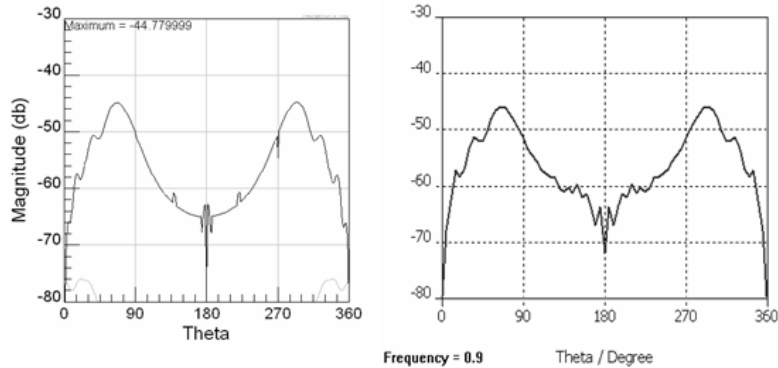


Figure 11. Far field (E-field) calculated in HF sub-domain using BSC code (left) compared to that from CST (right).

3. CONCLUSION

A strategy to design antennas under electrically large structures is presented by integrating simulation tools of NEC-BSC and CST, which are based on numerical high and low frequency techniques, respectively. An interface based on an equivalent current technique is established to interact and provide seamless transformations of parameters between the codes. Numerical examples demonstrate the validity of the proposed work.

ACKNOWLEDGMENT

This work is financially sponsored by National Science Council, Taiwan under contract no. 96-2623-7-155-002-D. The authors would like to acknowledge Nearson Marketing Group (NMG), Taiwan for support of CST Design Studio 2006B license for simulation.

REFERENCES

1. Chen, M., X.-W. Zhao, Y. Zhang, and C.-H. Liang, "Analysis of antenna around NURBS surface With iterative MOM-PO technique," *Journal of Electromagnetic Waves and Applications*, Vol. 20, No. 12, 1667–1680, 2006.
2. Ding, W., Y. Zhang, P. Y. Zhu, and C. H. Liang, "Study on electromagnetic problems involving combinations of arbitrarily oriented thin-wire antennas and inhomogeneous dielectric objects

- with a hybrid MOM-FDTD method,” *Journal of Electromagnetic Waves and Applications*, Vol. 20, No. 11, 1519–1533, 2006.
3. Zhang, Y.-I. and E.-P. Li, “Scattering of three-dimensional chiral objects above a perfect conducting plane by hybrid finite element method,” *Journal of Electromagnetic Waves and Applications*, Vol. 19, No. 11, 1535–1546, 2005.
 4. Volakis, J. L., A. Chatterjee, and L. C. Kempel, *Finite Element Method for Electromagnetics: Antennas, Microwave Circuits, and Scattering Applications*, 368, IEEE Press and Oxford University Press, New York, 1998.
 5. Taflove, A., “Application of the finite-difference time-domain method to sinusoidal steady state electromagnetic penetration problems,” *Electromagnetic Compatibility, IEEE Transaction*, Vol. 22, 191–202, 1980.
 6. Harrington, F. F., *Computation by Moment Methods*, Macmillan, New York, 1968.
 7. Kouyoumjian, R. G. and P. H. Pathak, “A uniform geometrical theory of diffraction for an edge in a perfectly conducting surface,” *Proceedings of the IEEE*, Vol. 62, No. 11, 1448–1461, Nov. 1974.
 8. Ufimtsev, P. Y., *Method of Edge Waves in the Physical Theory of Diffraction*, Wiley-IEEE Press, February 16, 2007.
 9. Tiberio, R., S. Maci, and A. Toccafondi, “An incremental theory of diffraction: electromagnetic formulation,” *IEEE Transactions on Antennas and Propagation*, Vol. 43, No. 1, 87–96, Jan. 1995.
 10. Chen, M., Y. Zhang, and C. H. Liang, “Calculation of the field distribution near electrically large NURBS surfaces with physical-optics method,” *Journal of Electromagnetic Waves and Applications*, Vol. 19, No. 11, 1511–1524, 2005.
 11. Zhang, P. F. and S. X. Gong, “Improvement on the forward-backward iterative physical optics algorithm applied to computing the RCS of large open-ended cavities,” *Journal of Electromagnetic Waves and Applications*, Vol. 21, No. 21, 457–469, 2007.
 12. Attiya, A. M. and E. El-Diwany, “A time domain incremental theory of diffraction: Scattering of electromagnetic pulsed plane waves,” *Progress In Electromagnetics Research*, PIER 44, 81–101, 2004.
 13. Attiya, A. M. and E. El-Diwany, “Scattering of X-waves from a circular disk using a time domain incremental theory of diffraction,” *Progress In Electromagnetics Research*, PIER 44, 103–129, 2004.

14. Attiya, A. M. and E. El-Diwany, "Diffraction of a Transverse Electric (TE) X-wave by conducting objects," *Progress In Electromagnetics Research*, PIER 38 167–198, 2002.
15. Chen, X. J. and X. W. Shi, "Backscattering of electrically large perfect conducting targets modeled by NURBS surfaces in half-space," *Progress In Electromagnetics Research*, PIER 77 215–224, 2007.
16. Ruppin, R., "Scattering of electromagnetic radiation by a perfect electromagnetic conductor cylinder," *Journal of Electromagnetic Waves and Applications*, Vol. 20, No. 13, 1853–1860, 2006.
17. Thiele, G. A. and T. H. Newhouse, "A hybrid technique for combining moment methods with the geometrical theory of diffraction," *IEEE Trans. Antennas Propagat.*, Vol. AP-23, No. 1, Jan. 1975.
18. Burnside, W., C. Yu, and R. Marhefka, "A technique to combine the geometrical theory of diffraction and the moment method," *IEEE Transactions on Antennas and Propagation*, Vol. 23, Issue 4, 551–558, Jul. 1975.
19. Fourie, A. and D. Nitch, "SuperNEC: antenna and indoor-propagation simulation program," *IEEE Antennas and Propagation Magazine*, Vol. 42, Issue 3, 31–48, June 2000.
20. Davidson, D. B., I. P. Theron, U. Jakobus, F. M. Landstorfer, F. J. C. Meyer, J. Mostert, and J. J. Van Tonder, "Recent progress on the antenna simulation program FEKO," *Communications and Signal Processing, 1998. COMSIG '98. Proceedings of the 1998 South African Symposium*, 427–430, Sept. 7–8, 1998.
21. Stupfel, B. and M. Mognot, "A domain decomposition method for the vector wave equation," *IEEE Transactions on Antennas and Propagation*, Vol. 48, Issue 5, 653–660, May 2000.
22. NEC-BSC version 4.2 User's Manual, The Ohio State University, June 2000.
23. CST Studio Suite 2006B User's Manual, CST Computation Simulation Technology, 2006.
24. Clemens, M., S. Feigh, and T. Weiland, "Geometric multigrid algorithms using the conformal finite integration technique," *IEEE Transactions on Magnetics*, Vol. 40, Issue 2, Part 2, 1065–1068, March 2004.
25. Garcia-Pino, A., F. Obelleiro, and J. L. Rodriguez, "Scattering from conducting open cavities by generalized ray expansion (GRE)," *IEEE Transactions on Antennas and Propagation*, Vol. 41, Issue 7, 989–992, July 1993.